ELSEVIER

Physica D 128 (1999) 224–235

PHYSICA D

Interaction of chaotic rotating waves in coupled rings of chaotic cells

I.P. Mariño [a,*], V. Pérez-Muñuzuri [a], V. Pérez-Villar [a], E. Sánchez [b], M.A. Matías [c]

[a] *Group of Nonlinear Physics, Faculty of Physics, University of Santiago de Compostela, 15706 Santiago de Compostela, Spain*
[b] *Escuela Técnica Superior de Ingeniería Industrial, Universidad de Salamanca, E-37700 Béjar, Salamanca, Spain*
[c] *Física Teórica, Facultad de Ciencias, Universidad de Salamanca, E-37008 Salamanca, Spain*

Received 24 August 1998; accepted 24 November 1998
Communicated by Y. Kuramoto

Abstract

The interaction of two chaotic rotating waves of the type recently reported by Matías et al. [Europhys. Lett. 37 (1997) 379] is studied experimentally with arrays of non-linear electronic circuits arranged in ring geometries. Unidirectional coupling is assumed for the cell-to-cell coupling within the same ring, but between rings, cells are coupled diffusively. Depending on the relative sense of driving, competition between a rotating chaotic wave and a global synchronized state has been observed. The results are rationalized by means of a linear stability analysis around the uniform synchronized behavior, where the circulant symmetry of the system allows to express the problem as a superposition of a series of Fourier modes.

PACS: 05.45.+b; 47.20.Ky; 03.40.Kf; 84.30.Bv

1. Introduction

The present work continues our research line on pattern formation arising from instabilities in the uniform synchronized state of small assemblies of chaotic non-linear analog oscillators [1–4]. In particular, in [2] we found that N Chua's oscillators, coupled unidirectionally by using a method introduced in [5] as a generalization of Pecora–Carroll synchronization through driving method, and with a ring arrangement, develop an instability that leads to the appearance of *chaotic rotating waves*, that are characterized by a chaotically varying amplitude and an approximate phase relationship between neighbor oscillators of $2\pi/N$. Moreover, in [4] we were able to confirm experimentally the existence of this new type of waves, that are complex spatio-temporal structures that form in a discrete medium [6] with local chaotic dynamics. In the present contribution, we shall consider the situation in which there are two such rings (where coupling goes unidirectionally) that are transversally coupled (bidirectionally). The result is a complex interaction between the chaotic rotating waves in each ring, that we analyze through a linear stability analysis.

* Corresponding author. E-mail: uscfmipm@cesga.es.

0167-2789/99/$ – see front matter
PII: S0167-2789(98)00303-0

Rings of coupled (discrete) cells are relevant in the study of some physiological and biochemical systems. Thus, one has the seminal work by Turing [7,8], who used this kind of system in his proposal of a plausible model of morphogenesis. Later, this kind of models were used to study slow-wave activity in the mammalian intestine [9]. More interesting, perhaps, is the interest on these systems in the context of neural systems, namely in the context of central pattern generators (CPGs) [10]. These are networks of neurons in the central nervous system capable of producing an autonomous rhythmic output (breathing, walking, running, etc.), i.e., without making use of sensory feedback with the corresponding moving organ. Although current neurophysiological techniques are unable to isolate such circuits among the intricate neural connections of complex animals, there are some strong indirect experimental evidences (see, e.g. [11–13]). Moreover, rings of coupled electronic oscillators, CPG-like, are an interesting method in the design and control of legged robots, because they produce a variety of phase relationships in a stable and natural manner [14]. An interesting study is that of Collins and Stewart [15,16] who, in the case of animals with a small number of legs, obtained the patterns of oscillations (i.e. the gaits) used by these animals in their locomotion [17]. They did so by analyzing the periodic states that arise through a symmetric Hopf bifurcation [18] from the trivial *stand* gait and by using simple symmetric networks of coupled identical cells.

Although rings are a useful way of implementing CPGs, it happens that one cannot obtain all the gaits (phase relationships) from a single ring of coupled oscillators, whose symmetry, connectivity, etc. are fixed. Thus, it is natural to think about extending the simplest ideas by considering more complex networks of coupled oscillators. A possible extension consists of assemblies of $2N$ identical oscillators in which the CPG is composed out by two rings, where oscillators within a ring have identical unidirectional coupling, while the two rings are coupled transversally by a different type of coupling (bidirectional). In this way one has probably a more realistic representation of CPGs of bilaterally symmetric animals, that, hopefully, will describe more accurately locomotion in these animals. Among the studies of CPGs similar to the one we are studying here one can mention the study of Collins and Stewart [15], who considered two coupled rings each comprising three oscillators and that of Ermentrout and Kopell [19]. A recent important study related to our work was carried out by Golubitsky et al. [20], who proposed a modular symmetric network consisting of two mutually coupled rings, each one made of $2N$ identical cells coupled unidirectionally to reproduce the phase relationships found in gaits of a $2N$-legged animal. In addition, one could consider more complex networks, where one can mention the modeling of the human colon in [21], which consists of 33 symmetrically coupled three-membered rings.

In studying and modeling CPGs one has to consider not just the topology and detailed form of connections but also the local dynamics of the oscillators. Although most of the studies [15,16,20] consider a quiescent or periodic local dynamics, it is important to recall that experiments performed in recent years indicate that normal activity of a single, i.e. isolated, neuron is deterministic chaos [22–24]. Leaving aside questions of the type of how this internal chaotic dynamics manifests in a CPG as a periodic (or, at least, more regular) behavior, in the present work we extend our previous studies [1,2,4] in which we studied rings of chaotic oscillators with unidirectional coupling to the case of two rings that are coupled transversally through resistive, i.e. diffusive, coupling. In particular, we shall study non-linear electronic (analog) oscillators capable of chaotic behavior as a simplified representation of the local (neuronal) dynamics. Analogously to what happens in the case of single rings [2,4] the behavior of the system is synchronized chaos below a certain parameter value and/or system size, while a desynchronizing bifurcation occurs above some threshold. In particular, in the case of the oscillators that we are considering a chaotic rotating wave that travels through the system appears. As this structure appears in each ring, our study will consist mainly in the interaction of these structures between the two rings, interaction that leads to richer spatio-temporal structures.

2. Experimental results

Experiments have been performed with two boards each one containing up to six Chua's circuits [25] in the chaotic regime, according to the design introduced in [4,26]. The components of the circuits are defined by parameters C_1, C_2, L, r_0 and R whose values are 10 nF, 100 nF, 10 mH, 20 Ω, 1.1 kΩ. The circuits were sampled with a digital oscilloscope (Hewlett-Packard 54601) with a maximum sampling rate of 20 million samples per second, 8 bit A/D resolution, and a record length of 4000 points. The six circuits of each board were connected unidirectionally through driving [4,5] and in a ring geometry, i.e., the arrangement is such that the last circuit drives the first one. Besides, both rings were connected, cell-to-cell, through resistances, R_c, from the C_1 capacitors of the corresponding cells, leading to a diffusion term in the potential differences [6]. Numerical simulations with Spice [27], where a detailed description of the non-linear element is implemented were used to complete the experimental results.

The evolution equations for a single circuit in the whole setting can be obtained from the application of Kirchhoff's laws in the form,

$$\begin{aligned} C_1\frac{\mathrm{d}V^i_{1,j}}{\mathrm{d}t} &= \frac{V^i_{2,j}-V^i_{1,j}}{R} - g(\overline{V^i_{1,j}}) + \frac{V^{i+1}_{1,j}-V^i_{1,j}}{R_c},\\ C_2\frac{\mathrm{d}V^i_{2,j}}{\mathrm{d}t} &= \frac{V^i_{1,j}-V^i_{2,j}}{R} + I^i_{L,j},\\ L\frac{\mathrm{d}I^i_{L,j}}{\mathrm{d}t} &= -V^i_{2,j} - I^i_{L,j}r_0, \end{aligned} \tag{1}$$

with $j = 0, \ldots, (N-1)$ runs over the number of elements in the ring, and where $i = 0, 1$ runs over the number of coupled rings. Coupling within each ring enters in the non-linear element, as the corresponding term, $g(\overline{V_{1,j}})$, is not driven, in principle, by the voltage across capacitor C_1 of the jth circuit, but by the voltage across capacitor C_1 of a different circuit of the same ring. The precise driving circuit depends on the type of coupling, as we have found this ordering more convenient in the theoretical treatment to be discussed later.

Two different configurations of the setup have been analyzed in the present work: (1) cells within a ring were unidirectionally coupled in the same direction (parallel coupling); (2) cells within a ring were unidirectionally coupled in opposite directions (antiparallel coupling). Thus, for parallel coupling $\overline{V^i_{1,j}} = V^i_{1,j-1}$, for both $i = 0, 1$, while for antiparallel coupling this voltage will be different for the two rings: for one of them, say $i = 0$, it has the same value, i.e., $\overline{V^0_{1,j}} = V^0_{1,j-1}$, while the other one gets $\overline{V^1_{1,j}} = V^1_{1,j+1}$, where the operations in j indices are modulo N and in i indices are modulo 2. Besides, only the limit of strong coupling between rings will be studied here.

For weak coupling, rotating waves do not see each other, and the observed behavior corresponds to two non-interacting waves. Fig. 1 shows the chaotic rotating wave that develops in each ring when uncoupled, and that corresponds to the observed waves for a single ring [2,4]. This wave can be characterized by looking at the simultaneous representation of the voltages across one capacitor, say C_1, versus time for several consecutive circuits Fig. 1(a). This allows to see the *fingerprint* of these waves more clearly: they are waves where one has a modulated envelope, with an aperiodic frequency, indicating the superposition of several modes, that includes waves with an approximate phase relationship of $2\pi/N$, with N the number of oscillators, that is six in our case. In turn, Fig. 1(b) contains a representation of the voltages across capacitor C_2 corresponding to two contiguous circuits in the same ring, while in Fig. 1(c) the voltage across capacitor C_1 is represented versus the voltage across capacitor C_2, both corresponding to the same circuit. This rotating wave within each ring will be the initial state before coupling in the subsequent studies.

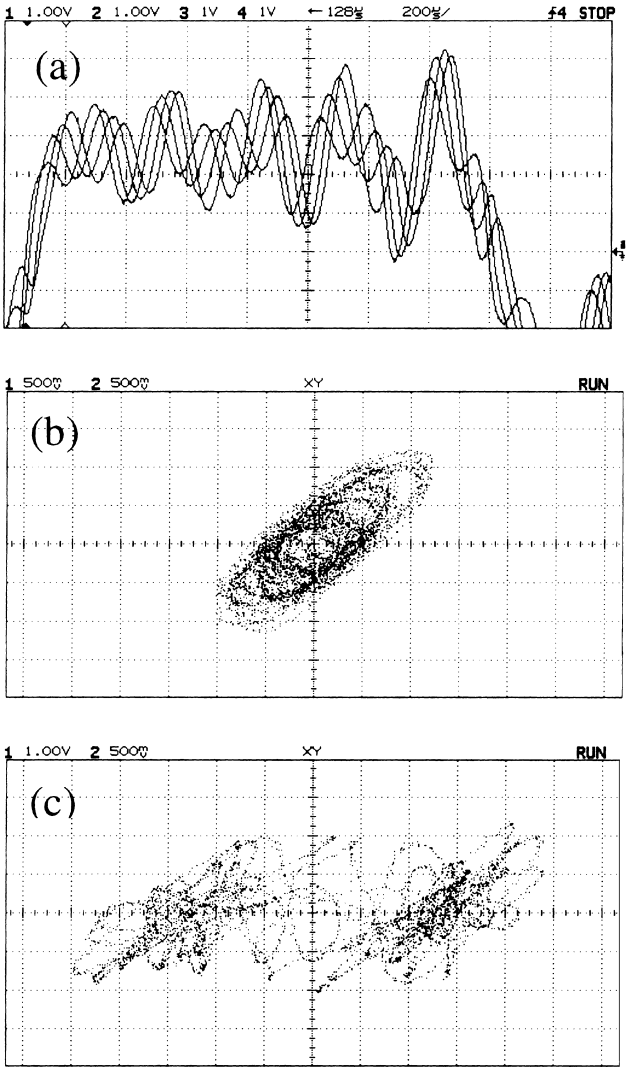

Fig. 1. Experimental results for a ring of six Chua's circuits unidirectionally coupled. (a) Time series of the voltage at the capacitor C_1 in four contiguous circuits; (b) representation of voltages at capacitors C_2 in two contiguous circuits one as a function of the other one and (c) phase plane of the two voltages at both capacitors of one circuit.

The observed behavior is that lateral (resistive) coupling introduces a further instability that, in the simplest case, i.e., two parallel rings, yields a transition between synchronized behavior between the two rings and desynchronized behavior. In both cases, each ring exhibits a chaotic rotating wave behavior. In a way the behavior is quite predictable: for values of $R_c < R_{th}$ (strong coupling), the two chaotic rotating waves synchronize with each other, while for values of $R_c > R_{th}$ (weak coupling) the two rotating waves become just uncorrelated to each other. This means that synchronization implies that homologous circuits, i.e., those circuits, one from each ring, that are coupled directly through a resistance are synchronized to each other, but exhibit the well-known $2\pi/N$ phase relationship with neighboring circuits. Or, in other words, what one gets in the strong coupling limit is a reduction in dimensionality of the behavior of the $2N$-sized ring in state space (of dimension $6N$): it collapses to a synchronization manifold

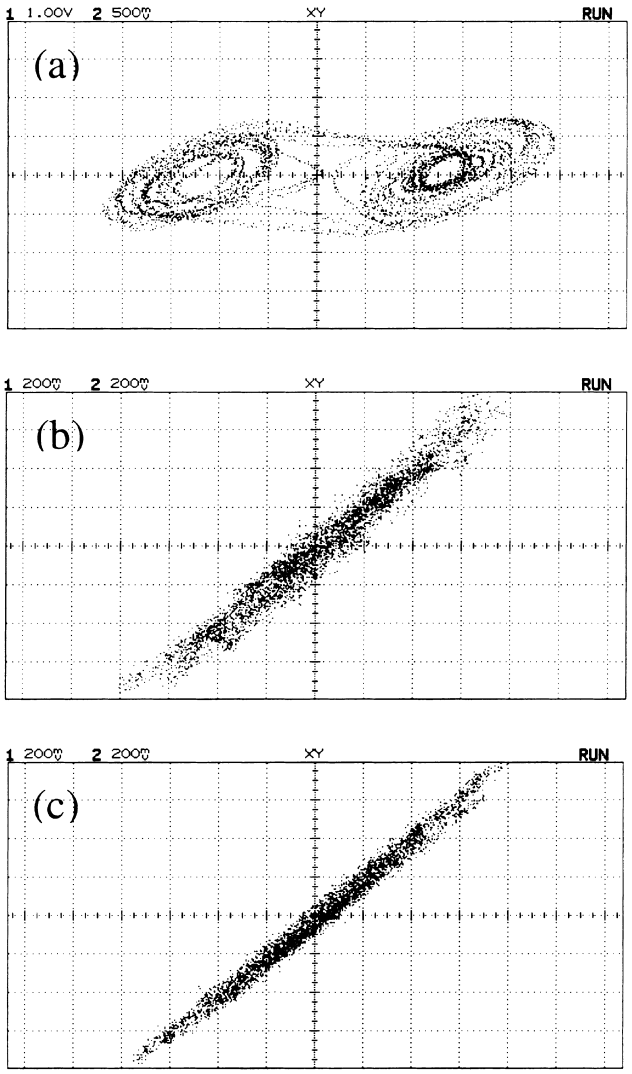

Fig. 2. Double-scroll synchronization for two rings in opposite sense of driving diffusively coupled cell-to-cell for $R_c = 1\,\Omega$. (a) Phase plane of two voltages at both capacitors of one circuit showing the classical Chua's double-scroll chaotic attractor, (b) representation of voltages at the same capacitor for two contiguous circuits of the same ring and (c) for opposite rings.

corresponding to a chaotic rotating wave for the N-sized ring (of dimension $3N$). In this context, the coupling resistance R_c plays the role of the inverse of the diffusion or coupling coefficient.

Quite different (and much richer) is the observed behavior for rings arranged in antiparallel sense. Thus, in the case of strong coupling all the circuits become synchronized and exhibit the well-known Chua's double-scroll chaotic attractor behavior (of course, the transition occurs at R_{th} value that is different to the one found for parallel rings). Thus, in this case the synchronization manifold has dimension 3. A phase portrait of this behavior, V_2 versus V_1 for a given circuit, is shown in Fig. 2(a), while in Fig. 2(b–c) we have represented voltage across capacitor C_2 for two contiguous circuits in the same ring and for two directly coupled circuits of different rings, respectively. Synchronized behavior can be deduced from the $y = x$ characteristic behavior, although with some thickness due to the fact that the circuits

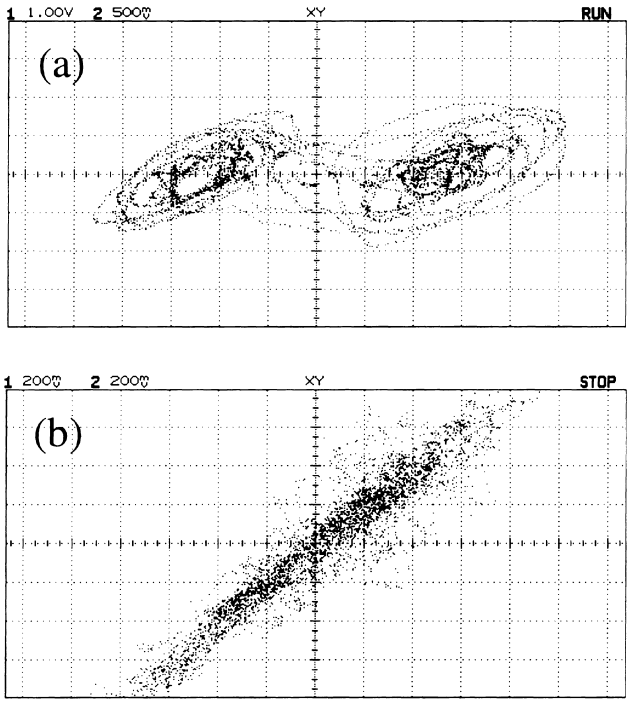

Fig. 3. Disturbed double-scroll chaotic attractor obtained for a value of $R_c = 27\,\Omega$. (a) Phase plane of two voltages at both capacitors of one circuit showing the transition from a double-scroll chaotic attractor to a chaotic rotating wave and (b) representation of voltages at the same capacitor for two contiguous circuits of the same ring. Notice that the captured image presented in panel (a) is a genuine effect and not a technical feature of the oscilloscope (see the label RUN in the right-top of the panel).

are not identical and also to the resistive coupling between circuits of different rings. When comparing to the case of a single isolated ring, antiparallel coupling delays the appearance of the instability in the two rings, that lead to a chaotic rotating wave.

The behavior changes as R_c is increased, basically because the globally synchronized double-scroll behavior loses stability when R_c is changed in this way. The fact that the uniform synchronized chaotic state is stable implies that the corresponding transverse Lyapunov spectrum (TLS) must be negative [28]. However, even when the largest transverse exponent is negative (although close to zero) interesting phenomena may occur [29], as during short periods of time it may become positive (this exponent is guaranteed to be negative only in the asymptotic limit). In particular, the behavior that we get in our system is very close to an on–off intermittency [30], that in our case, manifests in that the double-scroll attractor appears to be *alive* and *breath*. The system is subject to perturbations, not withstanding which, they are not able to induce a transition to a different behavior. This type of situation can be observed in Fig. 3(a–b) . Notice the coexistence in time of both kinds of attractors, namely, the double-scroll and the rotating wave shown in Fig. 3(a). The most striking aspect of this behavior is that typical lifetimes of each of the two transient states may be up to a few minutes, what is quite uncommon in this type of electronic analog circuits, with usual characteristic times of the order of the milliseconds. However, the transition itself is very fast. Moreover, the blurring in the characteristic $y = x$ line shown in Fig. 3(b) implies that the double-scroll synchronized state is contaminated by perturbations, that resemble the characteristic Lissajoux-type figure of a chaotic rotating wave.

3. Theoretical analysis

As in our previous contributions [1,2,4], we shall analyze the experimental results presented in Section 2 by performing a linear stability analysis around the (global) synchronized state. In the theoretical study, and as in the previous work [2,26] we shall consider a dimensionless version of Eq. (1), that allows us to write the following evolution equations,

$$\begin{aligned}
\dot{x}^i_j &= \alpha[y^i_j - x^i_j - f(\overline{x}^i_j)] + D(x^{i+1}_j - x^i_j),\\
\dot{y}^i_j &= x^i_j - y^i_j + z^i_j,\\
\dot{z}^i_j &= -\beta\, y^i_j - \gamma\, z^i_j,
\end{aligned} \tag{2}$$

where the non-linear element is given by $f(x^i) = \{bx^i + (1/2)(a-b)[|x^i+1| - |x^i-1|]\}$, and again, and as explained in Eq. (1), $j = 0, \ldots, (N-1)$ runs over the number of elements in the ring, and $i = 0, 1$ is the index of ring, and, again, for parallel coupling $\overline{x}^i_j = x^i_{j-1}$ for both $i = 0, 1$, while in the case of antiparallel coupling $\overline{x}^0_j = x^0_{j-1}$ and $\overline{x}^1_j = x^1_{j+1}$, where the operations over the j indices are modulo N and over the i indices modulo 2. The coupling constant D is proportional to the inverse of the coupling resistance.

The stability analysis of the problem around the chaotic globally synchronized state starts by performing an expansion of Eq. (2) around the chaotic state [28,29] $(x_s(t), y_s(t), z_s(t))$, and keeping only linear terms, one obtains a set of $2N$-coupled differential equation system for all the $(\delta x, \delta y, \delta z)$, with a quite sparse structure, as it has $2N$ blocks of dimension 3×3 that correspond to the local dynamics of each cell, plus a (small) number of off-block-diagonal terms. The way of tackling this problem is different depending on the type of coupling between the rings: parallel or antiparallel.

3.1. Parallel coupling

In the first case the resulting matrix has a circulant structure, and can be put in block-diagonal form by applying a discrete Fourier transform (DFT) [7,28], as we did already for a single ring of Chua's cells [2,26]. The simplest way is probably to order the cells in such a way that one puts alternatively cells corresponding to Ring 1 and 2 that are resistively coupled together. We shall write the linearized problem in a more compact way by representing the variables of the problem in the form: $\delta\boldsymbol{x}^i_j = (\delta x^i_j, \delta y^i_j, \delta z^i_j)$, where these variables represent differences between neighbor circuits,

$$\begin{pmatrix} \delta\dot{\boldsymbol{x}}^0_0 \\ \delta\dot{\boldsymbol{x}}^1_0 \\ \delta\dot{\boldsymbol{x}}^0_1 \\ \delta\dot{\boldsymbol{x}}^1_1 \\ \cdots \\ \delta\dot{\boldsymbol{x}}^0_{N-1} \\ \delta\dot{\boldsymbol{x}}^1_{N-1} \end{pmatrix} = \begin{pmatrix} \boldsymbol{H}_0 & \boldsymbol{H}_1 & \boldsymbol{0} & \boldsymbol{0} & \cdots & \boldsymbol{H}_2 & \boldsymbol{0} \\ \boldsymbol{H}_1 & \boldsymbol{H}_0 & \boldsymbol{0} & \boldsymbol{0} & \cdots & \boldsymbol{0} & \boldsymbol{H}_2 \\ \boldsymbol{H}_2 & \boldsymbol{0} & \boldsymbol{H}_0 & \boldsymbol{H}_1 & \cdots & \boldsymbol{0} & \boldsymbol{0} \\ \boldsymbol{0} & \boldsymbol{H}_2 & \boldsymbol{H}_1 & \boldsymbol{H}_0 & \cdots & \boldsymbol{0} & \boldsymbol{0} \\ \cdots & \cdots & \cdots & \cdots & \cdots & \cdots & \cdots \\ \boldsymbol{0} & \boldsymbol{0} & \boldsymbol{0} & \boldsymbol{0} & \cdots & \boldsymbol{H}_0 & \boldsymbol{H}_1 \\ \boldsymbol{0} & \boldsymbol{0} & \boldsymbol{0} & \boldsymbol{0} & \cdots & \boldsymbol{H}_1 & \boldsymbol{H}_0 \end{pmatrix} \cdot \begin{pmatrix} \delta\boldsymbol{x}^0_0 \\ \delta\boldsymbol{x}^1_0 \\ \delta\boldsymbol{x}^0_1 \\ \delta\boldsymbol{x}^1_1 \\ \cdots \\ \delta\boldsymbol{x}^0_{N-1} \\ \delta\boldsymbol{x}^1_{N-1} \end{pmatrix}, \tag{3}$$

where the structure of the terms is as follows:

$$\boldsymbol{H}_0 = \begin{pmatrix} -\alpha - D & \alpha & 0 \\ 1 & -1 & 1 \\ 0 & -\beta & -\gamma \end{pmatrix}; \quad \boldsymbol{H}_1 = \begin{pmatrix} D & 0 & 0 \\ 0 & 0 & 0 \\ 0 & 0 & 0 \end{pmatrix}; \quad \boldsymbol{H}_2 = \begin{pmatrix} -\alpha f'(x) & 0 & 0 \\ 0 & 0 & 0 \\ 0 & 0 & 0 \end{pmatrix}. \tag{4}$$

The structure of the matrix in Eq. (3) is clearly circulant, where one has N number of 6×6 blocks whose structure repeats in the matrix. The problem can be brought to 6×6 block-diagonal form by applying a DFT [7,28] (over the index k) to yield the interaction of N 6×6 Fourier modes, $k = 0, \ldots, (N-1)$. At the same time, the N 6×6 modes can be written in a simple form by applying a second DFT, in the Fourier index $m = 0, 1$, within each block. While the Fourier transform that yields index k corresponds to a given ring, the other one is associated to the symmetry corresponding to every resistively coupled pair of circuits. The final result is that the linearized evolution Eq. (3) can be cast in a set of 3×3 equations, in which the Fourier modes are decoupled,

$$\dot{\eta}^{(k,m)} = \boldsymbol{C}^{(k,m)}\, \eta^{(k,m)} \tag{5}$$

where the structure of each block can be written in the form

$$\boldsymbol{C}^{(k,m)} = \begin{pmatrix} -\alpha[1 + f'(x)e_k] + D(e_m - 1) & \alpha & 0 \\ 1 & -1 & 1 \\ 0 & -\beta & -\gamma \end{pmatrix}, \tag{6}$$

with $e_k = \exp(\mathrm{i}2\pi k/N)$ and $e_m = \exp(\mathrm{i}\pi m)$, being $k = 0, \ldots, (N-1)$ and $m = 0, 1$ the indices of Fourier modes of the system, with N the number of oscillators of each ring. $\eta^{(k,m)}$ is obtained after applying two DFTs (with the respect to indices $k = 0, \ldots, (N-1)$ and $m = 0, 1$) to $\delta \boldsymbol{x}^i_j$. The $(k, m) = (0, 0)$ Fourier mode represents the uniform global chaotic synchronized state of the coupled system and the stability of this state can be characterized by analyzing the transverse Lyapunov spectrum. Global (double-scroll) synchronization occurs only if all the transverse Lyapunov exponents (TLEs) are negative. It is important to notice that the $(k, 0)$ Fourier modes take the same value than the k modes of a single ring [2,4], while the modes $(k, 1)$ are associated with the coupling between rings. Fig. 4(a) shows the TLEs associated with Fourier modes $(k, 0)$ and $(k, 1)$. Note that for $N = 6$, the $(1, 0)$ mode is unstable, which corresponds to a chaotic rotating wave, since now the circuits are not synchronized inside each ring. As in [2], we warn that the predictions of this linear stability analysis give useful information only regarding the

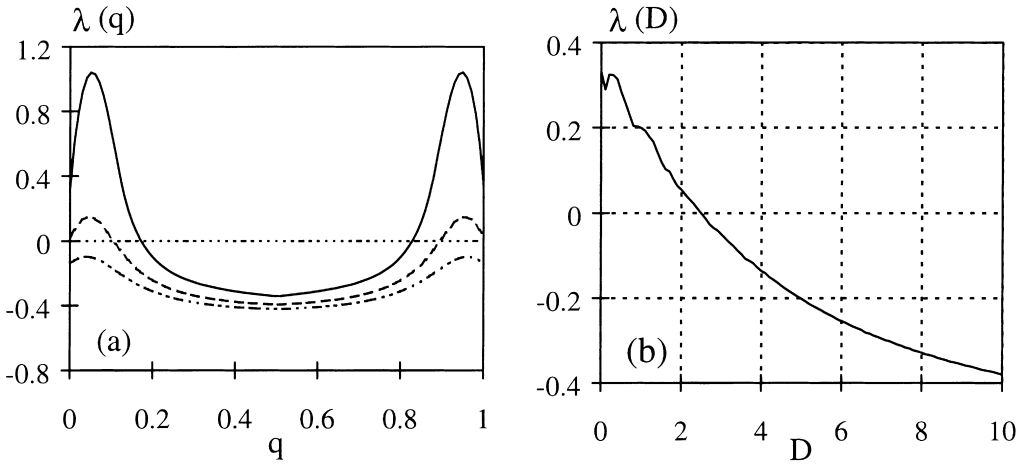

Fig. 4. (a) Representation of the highest transverse Lyapunov exponent, λ as a function of $q = k/N$ for two diffusively coupled rings with the same sense of driving. N is the total number of Chua's circuits in a ring and $k = 0, \ldots, N-1$ the Fourier modes associated with the size of the ring. The upper curve represents the highest TLE for the modes $(k, m) = (k, 0)$, which corresponds with the case of a single ring without coupling. The middle curve represents the highest TLE for the modes $(k, m) = (k, 1)$ when the coupling coefficient is $D = 2.3$. The lower curve represents the highest TLE for the modes $(k, m) = (k, 1)$ when the coupling coefficient is $D = 4$. (b) representation of the highest TLE for the mode $(k, m) = (0, 1)$ versus the coupling coefficient D. The value of the parameters for each circuit in Eq. (2) are: $(\alpha, \beta, \gamma, a, b) = (10, 12.1, 0.22, -1.26, -0.79)$.

onset of instability, not so much the final outcome of such instability, that depends also on higher non-linear terms in the expansion that are neglected in this level of approximation. The TLEs associated with modes $(k, 1)$ logically depend on the coupling coefficient D (see Eq. (6)). Thus, for strong enough coupling the linear theory shows that it is possible to obtain all the TLEs negative, which corresponds to the synchronization between chaotic rotating waves of different rings. Fig. 4(b) shows the dependence of the mode $(0, 1)$ with the coupling coefficient, showing the mentioned transition.

3.2. Antiparallel coupling

We shall now analyze the situation corresponding to antiparallel coupling. In this case it is more convenient to perform a different ordering of the cells, namely by grouping together those corresponding to the same ring, and the result that one gets is the following,

$$\begin{pmatrix} \delta\dot{\boldsymbol{x}}_0^0 \\ \delta\dot{\boldsymbol{x}}_0^1 \\ \delta\dot{\boldsymbol{x}}_1^0 \\ \delta\dot{\boldsymbol{x}}_1^1 \\ \dots \\ \delta\dot{\boldsymbol{x}}_{N-1}^0 \\ \delta\dot{\boldsymbol{x}}_{N-1}^1 \end{pmatrix} = \begin{pmatrix} \boldsymbol{H}_0 & \boldsymbol{H}_1 & \boldsymbol{0} & \boldsymbol{0} & \dots & \boldsymbol{H}_2 & \boldsymbol{0} \\ \boldsymbol{H}_1 & \boldsymbol{H}_0 & \boldsymbol{0} & \boldsymbol{H}_2 & \dots & \boldsymbol{0} & \boldsymbol{0} \\ \boldsymbol{H}_2 & \boldsymbol{0} & \boldsymbol{H}_0 & \boldsymbol{H}_1 & \dots & \boldsymbol{0} & \boldsymbol{0} \\ \boldsymbol{0} & \boldsymbol{0} & \boldsymbol{H}_1 & \boldsymbol{H}_0 & \dots & \boldsymbol{0} & \boldsymbol{H}_2 \\ \dots & \dots & \dots & \dots & \dots & \dots & \dots \\ \boldsymbol{0} & \boldsymbol{0} & \boldsymbol{H}_2 & \boldsymbol{0} & \dots & \boldsymbol{H}_0 & \boldsymbol{H}_1 \\ \boldsymbol{0} & \boldsymbol{H}_2 & \boldsymbol{0} & \boldsymbol{0} & \dots & \boldsymbol{H}_1 & \boldsymbol{H}_0 \end{pmatrix} \cdot \begin{pmatrix} \delta\boldsymbol{x}_0^0 \\ \delta\boldsymbol{x}_0^1 \\ \delta\boldsymbol{x}_1^0 \\ \delta x_1^1 \\ \dots \\ \delta\boldsymbol{x}_{N-1}^0 \\ \delta\boldsymbol{x}_{N-1}^1 \end{pmatrix}. \tag{7}$$

The main difference of the problem of antiparallel coupling Eq. (7) with the previous case of parallel coupling Eq. (3) is that in the present case, it is not possible to bring the problem to block-diagonal form, at least in an obvious way, to yield a 3×3 decoupled problem (that runs over $k = 0, \dots, (N-1)$ and $m = 0, 1$). However, in the present situation it is possible to apply a Fourier transform over the ring coordinates, but the simplification that one can attain is, at most, to a 6×6 problem in which the two cells of different rings that are resistively coupled together appear. The structure of the 6×6 problem is of the form

$$\dot{\eta}^{(k)} = \boldsymbol{D}^{(k)}\, \eta^{(k)} \tag{8}$$

where $\boldsymbol{D}^{(k)}$ has the form,

$$\boldsymbol{D}^{(k)} = \begin{pmatrix} \boldsymbol{E}^{(k)} & \boldsymbol{H}_1 \\ \boldsymbol{H}_1 & \boldsymbol{E}^{(k)\dagger} \end{pmatrix}, \tag{9}$$

where

$$\boldsymbol{E}^{(k)} = \begin{pmatrix} -\alpha[1 + f'(x)\, e_k] - D & \alpha & 0 \\ 1 & -1 & 1 \\ 0 & -\beta & -\gamma \end{pmatrix}, \tag{10}$$

where $\boldsymbol{E}^{(k)\dagger}$ is the complex conjugate of $\boldsymbol{E}^{(k)}$, and where the other symbols have the same meaning as in the previous study. The characterization of the instability has been performed in this case as a function of the coupling coefficient D (that is the inverse of the corresponding coupling resistance R_c). Notice that in this case (see, e.g. Fig. 5) the situation differs compared to the case of parallel coupling. Here, for $N = 6$, one gets a completely negative TLS for some values of D, corresponding to strong coupling, while in the case of parallel coupling, size instability

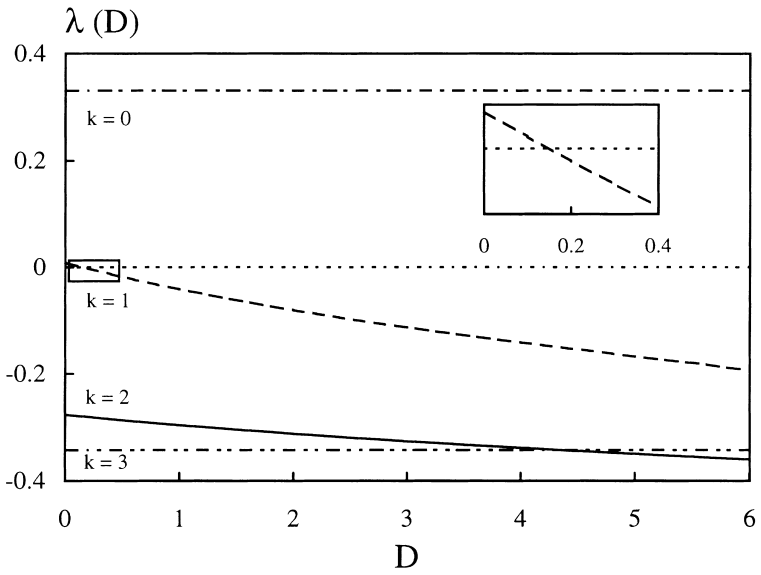

Fig. 5. Dependence of the highest Lyapunov Exponent $\lambda(D)$ corresponding to the modes $k = 0, \ldots, 3$ (for $N = 6$) on the coupling (diffusion) coefficient D between rings with opposite sense of driving. The inset shows the transition from positive to negative of the TLE corresponding to mode $k = 1$ for $D = 0.17$. Set of parameters as in Fig. 4.

effects within each ring dominated, leading to a chaotic rotating wave behavior, while resistive coupling lead just to synchronization between the two rings. This is due to the fact that due to the different sense of driving in each ring, the result of the DFT over the j indices of each ring, that yields the k wavenumbers, leads to nonidentical (complex conjugate) matrices. Thus, at variance to the parallel case discussed in the previous section, after the appropriate transformation to block-diagonal form none of the two 3×3 matrices is identical to that of a single ring (while this occurred for the $m = 0$ mode in the case of parallel coupling). The result is that both 3×3 matrices are shifted, when compared to those of a single ring, and for a range of values of D, this resistive transverse coupling is able to stabilize the TLS, yielding a globally synchronized chaotic state (as seen from Fig. 5). (Notice, however, that for the $k = 0$ mode one has an isolated Chua's circuit, as happens for a single ring.)

4. Conclusions

In the present work we have carried out a study of the behavior of coupled rings of cells with chaotic behavior. There is a lot of interest in this type of systems in neurobiology, as well as in practical applications like robotics. In particular, in the so-called CPGs, that are basically rings of neurons capable of autonomous rhythmic activity in response to a suitable stimulus. However, the direct physiological evidence of these structures is quite scarce, and, thus, one may expect that these CPGs are coupled and intertwined in complicated arrangements, that may affect to their dynamical behavior. In particular, in the present study we analyze the simplest situation involving the interaction of these CPG-like structures, namely, the case in which two of such rings interact. We consider the case in which the local dynamics of the cells is chaotic. As shown in our previous studies [2,4], this fact assures that the uniform synchronized state of the rings cannot be stable for arbitrary number of cells and/or coupling coefficients. An instability in this state must appear for some values of the parameters.

These instabilities lead to spatio-temporal (discrete) structures that travel over the assembly of cells. Transverse coupling between the rings guarantees interaction between the structures that appear within each ring. As the

coupling within each ring is unidirectional in our study, there are two possibilities in the way of coupling the two rings, depending on the sense of driving within each ring: parallel and antiparallel. The results of our study is that the observed behavior in these two cases is different, namely in the region of strong coupling.

Thus, in the case of parallel coupling one has two definite behaviors: if coupling is weak one has two desynchronized chaotic rotating waves, while if coupling is strong these two waves are synchronized between different rings. Instead, in the case of antiparallel coupling the situation is richer: for weak coupling one has (logically) the same behavior, namely, two desynchronized rings. On the other hand, curiously enough for strong coupling all the cells in the two rings become synchronized, being the behavior that corresponding to an isolated cell: a double-scroll. Thus, interestingly enough, transverse coupling is able to overcome the instability induced in a single ring by driving coupling [2,4].

We have explained these two different behaviors by performing a linear stability analysis around the uniform synchronized state for the two rings. In the case of parallel coupling it is possible to classify all the modes by using a second wavenumber $m = 0, 1$, in addition to the $k = 0, \ldots, (N-1)$ wavenumber. This simple fact implies that the instability corresponding to a single ring will be present as the the spectrum corresponding to the $m = 0$ mode is identical to that of a single ring, and if it has an instability for some wavenumber, typically for $k = 1$, this will dominate the whole system as the whole TLS (that corresponds to the modes $(k, m) \neq (0, 0)$) must be negative to obtain synchronization [28]. Instead, in the case of antiparallel coupling the crucial point is one does not get pure modes with a further wavenumber. However, transverse coupling mixes the different single ring modes that correspond to the two opposite senses in the two rings, and the transverse spectrum does not correspond to that of a single ring, being the effect of coupling stabilizing for strong coupling.

An interesting effect occurs for intermediate coupling, when the system exhibits a transition from uniform double-scroll behavior in the whole setting to two independent rotating waves. At some parameter region the system performs transitions between these two types of behavior, sometimes in a timescale that is larger than the typical timescale of the system by up to five orders of magnitude.

Acknowledgements

We thank C. Rico for his help on the experimental part of this work. This work was partially supported by *Dirección General de Enseñanza Superior* (DGES, Spain) under Research Grants No. PB95–0570 and PB97–0540, and by *Xunta de Galicia* and *Junta de Castilla y León* under Research Grants No. XUGA-20602B97 and SA31/97, respectively.

References

[1] M.A. Matías, V. Pérez-Muñuzuri, M.N. Lorenzo, I.P. Mariño, V. Pérez-Villar, Phys. Rev. Lett. 78 (1997) 219.
[2] M.A. Matías, J. Güémez, V. Pérez-Muñuzuri, I.P. Mariño, M.N. Lorenzo, V. Pérez-Villar, Europhys. Lett. 37 (1997) 379.
[3] I.P. Mariño, M.A. Matías, V. Pérez-Muñuzuri, , Int. J. Bif. and Chaos 8 (1998) 1733.
[4] E.Sánchez, M.A. Matías, V. Pérez-Muñuzuri, IEEE Trans. Circuits Syst. I, 1999, in press.
[5] J. Güémez, M.A. Matías, Phys. Rev. E 52 (1995) R2145.
[6] L.O. Chua (Ed.), Spatio-temporal patterns in electronic systems, IEEE Trans. Circuits Syst. I 42 (10) (1995).
[7] A.M. Turing, Phil. Trans. Roy. Soc. Lond. B 237 (1952) 37.
[8] J.D. Murray, Mathematical Biology, Chaps. 14, Springer, Berlin, 1989.
[9] D.A. Linkens, I. Taylor, H.L. Duthie, IEEE Trans. Biomed. Eng. 23 (1976) 101.
[10] R.M. Harris, E. Marder, A.I. Selverston (Eds.), Dynamic Biological Networks, MIT Press, Cambridge, 1992.
[11] S. Grillner, P. Wallén, Annu. Rev. Neurosci. 8 (1985) 233.
[12] S. Grillner, Science 228 (1985) 143.

[13] K.G. Pearson, Ann. Rev. Neurosci. 16 (1993) 265.
[14] S. Grillner, Sci. Am. 274(1) (1996) 48.
[15] J.J. Collins, I.N. Stewart, J. Nonlinear Sci. 3 (1993) 349.
[16] J.J. Collins, I.N. Stewart, Biol. Cybern. 35 (1994) 95.
[17] S.H. Strogatz, I.N. Stewart, Sci. Am. 269(6) (1993) 102.
[18] M. Golubitsky, I.N. Stewart, D.G. Schaeffer, Singularities and Groups in Bifurcation Theory, vol. II, Springer, New York, 1988.
[19] N. Kopell, G.B. Ermentrout, SIAM J. Appl. Math. 50 (1990) 1014.
[20] M. Golubitsky, I. Stewart, P.L. Buono, J.J. Collins, Physica D 115 (1998) 56.
[21] B.L. Bardakjian, S.K. Sarna, IEEE Trans. Biomed. Eng. 27 (1980) 193.
[22] H. Hayashi, S. Ishizuki, J. Theor. Biol. 156 (1992) 269.
[23] G.J. Mpitsos, R.M. Burton, H.C. Creech, S.O. Soinila, Brain Res. Bull. 21 (1988) 529.
[24] H.D.I. Abarbanel, M.I. Rabinovich, A. Selverston, M.V. Bazhenov, R. Huerta, M.M. Sushchik, L.L. Rubchinskii, Physics-Uspekhi 39 (1996) 337.
[25] R.N. Madan (Ed.), Chua's Circuit: A Paradigm for Chaos, World Science, Singapore, 1993.
[26] E. Sánchez, M.A. Matías, V. Pérez-Muñuzuri, Phys. Rev. E 56 (1997) 4068.
[27] R.M. Kielkowski, Inside Spice, McGraw-Hill, New York, 1994.
[28] J.F. Heagy, T.L. Carroll, L.M. Pecora, Phys. Rev. E 50 (1994) 1874.
[29] L.M. Pecora, T.L. Carroll, G.A. Johnson, D.J. Mar, J.F. Heagy, Chaos 7 (1997) 520.
[30] J.F. Heagy, N. Platt, S.M. Hammel, Phys. Rev. E 49 (1994) 1140.